Performance investigation of packed bed desiccant dehumidification system operating with aqueous lithium chloride

Mahesh Mahajan[1], **Mrinal Bhowmik**[1] **and P. Muthukumar**[1, 2, *]

[1] School of Energy Science and Engineering, Indian Institute of Technology Guwahati, Assam 781039, India.

[2] Department of Mechanical Engineering, Indian Institute of Technology Guwahati, Assam 781039, India.

[*]Corresponding author: Department of Mechanical Engineering, Indian Institute of Technology Guwahati, Assam 781039, India. *E-mail address:* pmkumar@iitg.ac.in

Abstract

Conventional air conditioning systems' dehumidification is an energy-intensive process due to the overcooling of air below its dew point temperature. In this regard, desiccant solution-based dehumidification is a promising alternative method for air dehumidification. The most prominent desiccant solutions are lithium bromide (LiBr), lithium chloride (LiCl), calcium chloride ($CaCl_2$), and tri-ethylene glycol (TEG). Amongst them, LiCl is the most commonly used desiccant due to its low vapor pressure characteristics. In the present study, the performance of the liquid desiccant-based air dehumidification system is studied numerically. The finite-difference model is adopted to estimate the thermodynamic properties of the liquid desiccant dehumidification system. The heat and mass transfer coefficients are calculated and discussed in detail. A particle model is used to study the pressure drop in the structured packing of the dehumidifier with LiCl and $CaCl_2$ solution. Different structured and random packing is compared based on the pressure drop value. The LiCl desiccant solution concentration is optimized using the statistical design of the experiments tool.

Keywords: Material Removal Rate, Response Surface Methodology, Lithium Chloride

1. Introduction/Background

In India, room AC sales demand has shown positive growth in between 2006 to 2017, where the demand was increased from 2 million units to 30 million units [1]. VCR system mostly uses the high global warming potential refrigerants such as R134A, R410a, R404A [2, 3]. India is the signatory of the Kigali agreement, in which India is supposed to reduce the use of its environment degrading refrigerants. It's prime time to look for alternative solutions for the VCR system, which is mostly a high-grade energy-consuming process. We need to look for a system that is more environment friendly and can operate on the low-grade energy, without compromising reliability and effectiveness [4]. Conventional VCR system if handling high value of latent heat can lead to the inefficient dehumidification process [5]. The most prominent alternative for the conventional dehumidification system is liquid desiccant-based dehumidification system. Liquid desiccant performs better compared to the solid desiccant based dehumidifier [6-8].

The dehumidifier performance predication is necessary. There are three basic models, which are used to predict the performance of the packed bed dehumidifier. The three models are namely finite difference model, NTU model and simplified model. In 1980 factor et al., [9] gave a model to predict the performance of the dehumidifier. This model was proposed for the counter current flow arrangements of packed bed columns. This model was based on the theory of Adiabatic gas absorption given by Treybal [10]. Only exception is that, the resistance to the heat transfer in the liquid phase is negligible and neglected [11]. NTU effectiveness model was modified from model for cooling towers [12, 13]. Simplified models are based on the experimental data collected to produce the empirical relations which are based on the input parameters. These performance parameters relations produced are sometimes system dependent and hence may not give accurate results.

In dehumidifier, the packing material creates obstruction for the flow of the air. Therefore, we need to see how much amount of energy is lost in making the circulation of the air in dehumidifier. When the packing is dry and when the desiccant is flowing, both conditions has different pressure drops. The pressure drop is increased when the liquid flows through that packing. This increase in the pressure drop, when the packing is irrigated is due to the fact that, liquid is being held up in the packing and this changes the effective structure of the bed; because of that porosity decreases [14]. Pressure drop in the packing is function of packing type, height, diameter of the packed bed and also depends on the desiccant and air mass flow rates [15]. There are basically three models to predict the pressure drop in the packed bed namely particle model, channel model, percolation model. In 1989 Stichlmair et al., [14] proposed a model to predict the pressure drop in the packed beds. This model was based on the particle theory in which the drag force on the hypothetical equivalent spheres were calculated. Channel model considers the uniformly distributed channels and flow in it and utilizes it to calculate the pressure drop in the packed bed. The increase in the air speed creates the holdup in the packing bed and a condition when pressure drop inside packing increases rapidly is called flooding. The percolation model uses the localized flooding concept. This model, when tested by Hanley et al. [16] in 1994, gave little different results than the experiments [16]. Castillo et al. [17] have used the model provided by Stichlmair et al. [14] and did some modifications for liquid holdup, irrigated and flooding pressure drop predication for random and structured packing. Koronaki et al. [18] have given the pressure drop equations and studied the pressure drop in the packed bed.

Heat and mass transfer coefficients drive the moisture transfer equations. These coefficients are derived from the experimental data and related with the dimensionless numbers. The equation given by Goswami et al. [11] gives the K type and F type mass transfer equation for the LiCl desiccant solution. The Chung and Ghosh et al. [19] gave equations for the heat and mass transfer equations and also was used in the Koronaki et al. [18] work. Gandhidasan et al. [20] has given the heat and mass transfer equations based on the effective velocities of the fluids.

Here, along with FDM model, the heat and mass transfer coefficient has been predicted numerically, considering the geometrical properties of the packing. The LiCl salt is costly and hence it is necessary to optimize its concentration in solution. Response surface methodology (RSM) is a statistical method with which we can optimize the concentration of the solution. This statistical tool has been used to calculate the optimum concentration for the desiccant solution. The system thermodynamic properties and pressure drop is calculated with the FDM model considering the geometrical parameters of the different packing materials, such as the specific surface area of the packing.

2. Numerical Methodology

2.1.1 Systems description for finite difference model

For the consideration of the problem, the work of Goswami et al. [11] is considered. The cylindrical dehumidifier column with 0.254 m diameter and 0.60 m height is considered. The packing material is Polypropylene Rauschert Hiflow Rings with surface area of 210 m^2/m^3. The desiccant solution considered is of LiCl salt. The model is iterated till the convergence criteria is met for the given inlet conditions and compared with the data from literature.

2.1.2 Assumptions in finite-difference model

- The flow of air and desiccant are assumed to be as slug flow.
- The adiabatic process is considered.
- The properties of the air and liquid desiccant solution are assumed to be constant.
- The heat and mass transfer area is equal to the packing material specific area.
- The concentration gradient and temperature gradient exists only in the z-direction.
- Non-uniformity in air motion is neglected.

2.1.3 Governing Equations in finite-difference model

In the model, the concentration gradient and temperature gradient exist only in the z-direction. Only the water is transferred between the air and the desiccant. The LiCl solution has the high surface tension and hence the insufficient area is wetted and therefore we need to consider this in the model. Equation to calculate the actual area is given by Onda et al. [22] and that equation is further used in the model for the calculation of the actual area.

$$a_w = a_t(1 - e^{-1.45\left(\frac{\sigma_c}{\sigma_L}\right)^{0.75} Re_L^{0.1} Fr_L^{-0.05} We_L^{0.2}}) \quad \text{(Eq.1)}$$

The below heat and mass transfer equations are used in the given dehumidifier model.

$$K_L = 0.0051\left(\frac{\mu_L g}{\rho_L}\right)^{0.3333}\left(\frac{L}{a_w \mu_L}\right)^{0.6667}\left(\frac{\rho_L D_L}{\mu_L}\right)^{-0.05}\left(a_t D_p\right)^{0.4} \quad \text{(Eq.2)}$$

$$K_G = 5.23\left(\frac{a_t D_G}{RT_a}\right)\left(\frac{G}{a_t \mu_G}\right)^{0.7}\left(\frac{\mu_G}{\rho_G D_G}\right)^{0.3333}\left(a_t D_p\right)^{-2} \quad \text{(Eq.3)}$$

$$ln\frac{1-Y_i}{1-Y} = ln\frac{1-\left(\frac{P_S}{P_t}\right)}{1-\left(\frac{P_a}{P_t}\right)} \quad \text{(Eq.4)}$$

$$h'_G a_t = \frac{-Gc_{p,v}\frac{dY}{dz}}{1-exp\left(\frac{Gc_{p,v}\frac{dY}{dz}}{a_t h_G}\right)};\ h_G = F_G M_a\left(c_{p,a} + Yc_{p,v}\right)\frac{Sc^{0.667}}{Pr^{0.667}};\ F_G = K_G P \quad \text{(Eq.5)}$$

The below equations are used to derive the values of the different thermodynamic properties and are iterated till the convergence criteria is met.

$$\frac{dY}{dZ} = -\frac{M_W F_G a_W}{G} ln\frac{1-Y_i}{1-Y} \quad \text{(Eq. 6)}$$

$$\frac{dT_a}{dz} = \frac{h'_G a_t (T_L - T_L)}{G(c_{p,a} + Yc_{p,v})} \quad \text{(Eq. 7)}$$

$$\frac{dL}{dz} = G\frac{dY}{dz};\quad \frac{dx}{dz} = -\frac{G}{L}x\frac{dY}{dz} \quad \text{(Eq. 8)}$$

$$\frac{dT_L}{dz} = \frac{G}{c_{p,L}L}\left\{\left(c_{p,a} + Yc_{p,v}\right)\frac{dT_a}{dz} + \left[\left(c_{p,v}(T_a - T_0) - c_{p,L}(T_L - T_0) + \varphi\right)\frac{dY}{dz}\right]\right\} \quad \text{(Eq. 9)}$$

Above all the equations are governed by the vapour pressure difference and it's the most important characteristics of the system. Above, all the equations are governed by the humidity differential element slope and which is further governed by the equilibrium humidity ratio at desiccant interface.

2.2 Pressure Drop Prediction

Structured packing results in lesser pressure drop compared to the random packing as per the Gandhidasan et al. [15] study. The desiccant flow rate does not have that much effect on pressure drop, as compared to the air flow rate. When the liquid flows through the packing materials the flow characteristics make the liquid to stay in the voids and this liquid is held inside the cavity and hence known as the dynamic holdup or operating holdup. When the air flow rate is significantly increased such that significant amount of liquid is held inside the packing, we call that point as the loading point of the packing. This loading decreases packing's area with increase in the liquid loading and void space becomes smaller. The point when the desiccant remains accumulated above the top side of packing we say that the packing is flooded. In this region, the pressure drop increases rapidly. The value of air flow rate at which this condition occurs, we call that point as the flooding point [15]. Stichlmair et al. [14] in their paper has used particle model for knowing the expected pressure drop in the packing. This model first predicts the dry pressure drop and then adds an extra arrangement for the pressure drop due to the liquid holdup. Castillo et al. [17] has used the model provided by Stichlmair et al. [14] and did some modifications for liquid holdup, irrigated and flooding pressure drop prediction [17].

2.2.1 Assumptions in the pressure drop model

- Inlet air velocity is assumed to be without variations or fluctuations.
- Thickness of the film formed over the packing is assumed to be constant.
- Properties of the air and desiccant are assumed to be constant throughout the packing.
- Equivalent diameter is assumed to be constant and is not varying with the liquid holdup.

2.2.2 Governing equations for the pressure drop model

From Treybal [10], we can get the equation for the equivalent diameter and it's given by:

$$D_P = \frac{6(1-\epsilon)}{a_t} \quad \text{(Eq. 10)}$$

The dry bed pressure drop is based on fluidized bed concept and it's given by following equation. Where, the friction factor depends on the type of the packing. This data for calculating the friction factor is given by the Stichlmair et al., [14] in their paper.

$$\Delta P_d = 0.125 f_0 \frac{\rho_G u_G^2 a_t}{\epsilon^{4.65}}; \quad f_0 = \frac{C_1}{Re_G} + \frac{C_2}{Re_G^{0.5}} + C_3; \quad Re_G = \frac{\rho_G D_P u_G}{\mu_G} \quad \text{(Eq. 11)}$$

The static and dynamic holdup is given by the following formula:

$$h_b = 3.6 \left(\frac{u_L a_t^{0.5}}{g^{0.5}}\right)^{0.66} \left(\frac{\mu_L a_t^{1.5}}{\rho_L g^{0.5}}\right)^{0.25} \left(\frac{\sigma_L a_t^{2.0}}{\rho_L g}\right)^{0.1}; \quad h_a = h_b \left[1 + \left(\frac{6\Delta P_{irri}}{\rho_L g}\right)^2\right] \quad \text{(Eq. 12)}$$

When we cross the loading point then the operating liquid holdup is the function of the irrigated or total pressure drop and which can be given by the following listed equations. In order to find the irrigated pressure, drop it is necessary to find the diameter of the falling liquid particles and that can be calculated by equating the surface tension force to the inertia force and it is given by the following equations:

$$d_L = C\sqrt{\frac{6\sigma_1}{(\rho_L - \rho_g)g}}; \quad a_L = 6\frac{h_a}{d_L} \quad \text{(Eq. 13)}$$

$$\frac{\Delta P_{irri}}{\Delta P_{dry}} = \left(\frac{a_L + a_t}{a_t}\right)\left(\frac{\epsilon}{\epsilon - h_a}\right)^{4.65} \quad \text{(Eq. 14)}$$

$$\Delta P_f = \frac{\rho_L g}{2988 h_b}\sqrt{249 h_b\left(\sqrt{X} - 60\epsilon - 558 h_b - 103 d_L D_P\right)} \quad \text{(Eq. 15)}$$

Constant C depends on structure of packing. Value of C is 0.8 and 0.4 for structured and random packing respectively. The above equations need to iterated to get the total pressure drop. Where flooding coefficient, X in the above equation can be calculated as follows:

$$X = 3600\,\epsilon^2 + 186500\,\epsilon h_b + 32300 d_L a_t \epsilon + 191800 {h_b}^2 + 95030 d_L a_t h_b + 10610 {d_L}^2 {a_t}^2 \quad \text{(Eq. 16)}$$

2.3 Volumetric heat and mass transfer coefficient

From above discussions and equations, we can get the clear view about importance of the heat and mass transfer coefficients and their usage in the moisture FDM model. Hence it is necessary to get the data of heat and mass transfer coefficients as accurate as possible. Ghosh and Chung have presented the data and equations for the coefficients, which they have derived from the dimensional analysis [19]. Here we are trying to verify the equations given by the Gandhidasan et al. [15]. They proposed equations for the both gas and liquid phase and for both random and structured packing material. Here we have tried to verify the equation for the structured packing. In their paper they have given the heat and mass transfer equations specially for the liquid phase along with the gas phase. These equations will be utilized in the future for further study.

2.3.1 Governing equations for the volumetric heat and mass transfer coefficient

The heat and mass transfer equations are governed by the effective velocities of the fluids in the packing. Effective velocities of fluid depend on the geometrical dimensions of the packing materials. The equations to calculate the effective velocity is given by the Gandhidasan et al. [20]. For all models, physical properties of the LiCl and $CaCl_2$ desiccant solution has been taken from the Conde et al. [22]. Heat and mass transfer equations for the gauze type structured packing are as follows:

$$h_{G,a} = 13.0 {U_{Le}}^{0.1} {U_{Ge}}^{0.79} e^{(-0.026 T_G)} \quad \text{(Eq. 17)}$$

$$F_{G,a} = 0.55 {U_{Le}}^{0.1} {U_{Ge}}^{0.79} e^{(-0.0293 T_G)} \quad \text{(Eq. 18)}$$

$$h_{L,a} = 15.1 {U_{Le}}^{0.4} {U_{Ge}}^{0.07} e^{(-0.031 T_L)} e^{(-0.003 x)} \quad \text{(Eq. 19)}$$

$$F_{L,a} = 8.2 {U_{Le}}^{0.4} {U_{Ge}}^{0.07} e^{(-0.038 T_L)} e^{(-0.009 x)} \quad \text{(Eq. 20)}$$

3. Results and discussion

3.1 Finite difference model validation

Nelson et al. [11] in their paper has considered the counter flow dehumidifier system. Here, they have used polypropylene Hi-flow rings having specific area of 210 m^2/m^3. Here they have given the experimental data; in which they have taken the data set of the average multiple experiments. Their input data for the dehumidifier is in the following table. Here we can see that the average error in the humidity prediction, concentration, air outlet temperature, desiccant outlet temperature is less than 7 %, 0.35%, 4%, 4.2%, respectively. The comparison of numerical data and experimental data is shown in the below table:

Table 1 Dehumidifier performance comparison with Goswami et al. [11] data

Experimental value (Goswami et al. [11])					**Model Predicted values**				
Y (kg/kg of dry air)	**X (fraction)**	**T_a ℃**	**T_L ℃**	**MRR (g/s)**	**Y (kg/kg of dry air)**	**X (fraction)**	**T_a℃**	**T_L ℃**	**MRR (g/s)**
0.0104	0.345	31.3	32.3	0.32	0.01117	0.35	30.33	30.87	0.275
0.0108	0.346	32.2	32.6	0.4	0.01183	0.347	30.40	31.23	0.335
0.0112	0.337	32.8	32.6	0.42	0.01108	0.344	34.63	31.36	0.415
0.0113	0.342	32.2	32.7	0.38	0.01209	0.343	30.42	31.30	0.318
0.011	0.343	32	32.5	0.39	0.01179	0.344	30.42	30.98	0.337
0.0114	0.33	32.4	32.2	0.36	0.012043	0.330254	30.19	30.97	0.31
0.0112	0.337	32.5	32.6	0.38	0.011893	0.337226	30.22	31.09	0.32
0.0107	0.347	32	32.5	0.41	0.011822	0.34717	30.31	31.13	0.33

3.2 Parametric study with finite difference model

3.2.1 Effect of the desiccant flow rate

As the solution flow rate increases, this increases the material removal rate (MRR) and the latent effectiveness (ε_{Lat}) of the solution. As the solution flow rate increases, this leads to decrease in the time the solution has to exchange the moisture from the air and hence the whole system remains at the initial system conditions. This increases the mass transfer potential and hence the MRR. The solution remains at the inlet conditions throughout the system and hence the output humidity ratio of air decreases; but the equilibrium ratio remains constant leading to increase in the effectiveness. After sufficient wetting of the packing material the effect of increase in the solution rate on MRR and Effectiveness is constant. This can be seen in figure 1.A which is given below.

3.2.2 Effect of the air flow rate

It can be seen from Fig. 1.B that with increase in the air flow rate; the MRR increases as it is directly proportional to the air flow rate. From Fig. 1.B it is evident that the effectiveness decreases as the velocity of the air increases. This is due to the fact that air has lesser time to interact with the solution and hence lesser potential to remove the humidity from the air. This decreases the output air humidity ratio with increase in the air flow rate as the cross-section of the flow remains constant. The equilibrium humidity ratio is constant, as it depends on the desiccant temperature and the concentration; so this decreases the effectiveness as it can be inferred from the latent effectiveness equation.

3.2.3 Effect of the desiccant temperature

With increase in the desiccant temperature the vapour pressure of the water at the interface increases. This increase in vapour pressure at the interface reduces the mass transfer potential decreasing the overall mass transfer characteristics as the temperature of inlet air is kept constant. With increase in the

desiccant temperature the equilibrium humidity ratio at the desiccant temperature will increase. This leads to the decrease in the denominator term of the effectiveness equation, which increases the overall effectiveness of the dehumidifier as the other parameters such as the concentration is kept constant. This can be seen in the below given Fig. 1.C where the MRR decreases and effectiveness increases with the increase in the desiccant temperature.

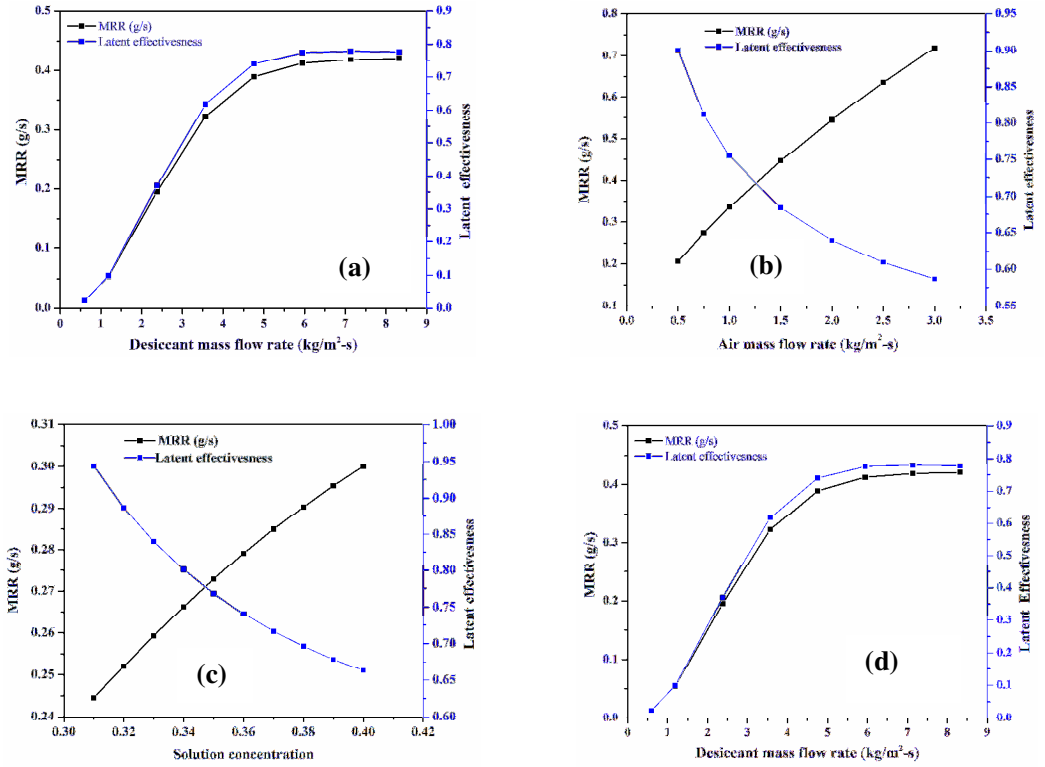

Figure 1 Parametric analysis of the finite difference model: effect of (a) desiccant mass flow rate on MRR and latent effectiveness (b) air mass flow rate on MRR and latent effectiveness (c) desiccant temperature on MRR and latent effectiveness (d) solution on MRR and latent effectiveness

3.2.4 Effect of the Desiccant Concentration

From figure 1.D, we can see that the effect of increasing the desiccant concentration is to increase the MRR and decrease the latent effectiveness. The vapor pressure at the desiccant air interface decreases with the increase in the desiccant concentration leading to increase in the vapour pressure difference between the air and desiccant solution ultimately increasing the driving force for mass transfer and hence the MRR increases with the increase in the concentration. The increase in the desiccant concentration leads to decrease in the equilibrium humidity ratio. Hence the denominator term in the effectiveness equation increases leading to decrease in the latent effectiveness of the system.

3.2 Pressure drop model validation

Koronaki et al. [18] has given equations and solved it for the pressure loss in the packing with LiCl desiccant solution. The following figure 2 compares the data from his paper and data from the model, made to predict the pressure drop when the air velocity is increased or the air flow rate is increased. It is obvious that as the air flow rate increases it will lead to increase in the liquid holdup, decreasing the flow area and hence reducing the actual void space. This enhances the air obstruction and hence the pressure drop increases with the increase in the air flow rate. From below figure 2, we can state that the value for the total pressure drop in Koronaki et al. [18] paper and prediction made by the model made here gives the good prediction, which matches with 2.5% error. From below figure 2.A it can be inferred that the total pressure drop increases with the increase in the air flow rate. When the given pressured

drop model was studied for the different packing's namely Raschig 15mm, Berl Saddles 35mm, Intalax saddles 35mm, Pall rings and Mellapak 250Y, Gempak 2A, the structured packing showed less pressure drop. The first generation random Raschig 15 mm packing showed the most drop in the pressure per unit length. While, the second generation Intalax saddle (having aerodynamic shape) and third generation pall rings showed the less pressured drop in the random packing's due to enhanced shape. The Mellapak 250Y and Gempak 2A has the least pressured drop amongst calculated packing. While, Mellapak 250Y has shown the least pressured drop in the structure and hence it is the most suitable packing material for the given application. Below given figure 2.B shows the relative comparison of the pressure drop in the different structures for $CaCl_2$ desiccant solution. The properties for the desiccant solutions were taken from the data provided by the Conde-petit et al., [22] researcher paper.

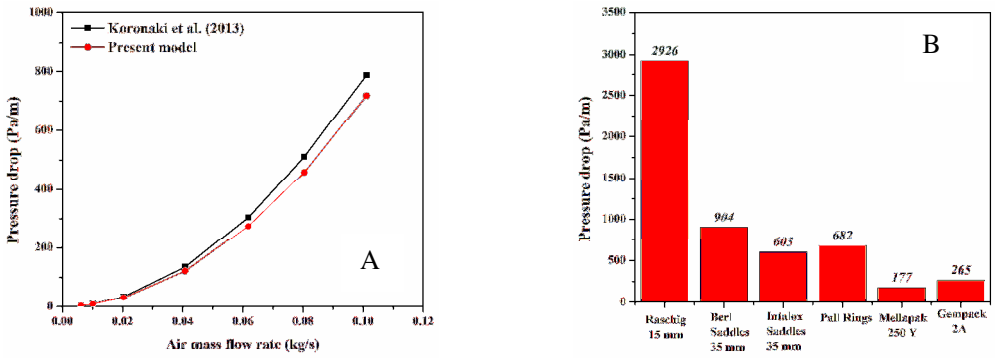

Figure 2.A Comparison of model-predicted values with Koronaki et al., [18] data with effect of variation of air flow rate (kg/s) on pressure drop (Pa/m) 2.B. Effect of different packing structures on pressure drop (Pa/m)

3.3 Volumetric heat and mass transfer coefficient equation results

The volumetric heat and mass transfer coefficient equations are given by Gandhidasan et al. [20], utilizes the effective velocity of liquid and gas phase. These equations also take into account the effect of temperature of the air and desiccant along with its concentration. This equation has been calculated with the conditions given in the paper. Here we have tried to reproduce the results for the both liquid and gas phase volumetric heat and mass transfer coefficient.

3.3.1 Variation of liquid volumetric mass transfer coefficient with liquid concentration

The volumetric mass transfer coefficient slightly increases with the increase in the concentration of the solution. As the concentration increases it leads to increase in the potential for the mass transfer by decreasing the interface surface vapour pressure. The effect of the increase in the value of the volumetric mass transfer coefficient with concentration is less compared to the effect of the flow rates. The average error in calculation of the volumetric mass transfer coefficient was around 0.3%. Below figure 3.A shows the variation of the predicted and paper value for the volumetric mass transfer coefficient with solution concentration.

3.3.2 Variation of liquid volumetric mass transfer coefficient with effective liquid velocity

Here the LiCl solution with 40% concentration, 10.5 m/s effective air velocity was kept constant. The effective liquid velocity was varied from 0.03 to 0.27 m/s, and the variation of the volumetric mass transfer coefficient was calculated. The results of the paper and the found data showed great similarities. The average error in predicting the coefficient was less than 0.3%. The variation of the Volumetric mass transfer coefficient for the liquid with liquid effective velocity is shown in Figure 3.B. It can be stated that the more the velocity of the liquid, more the mass transfer potential. The increase in velocity leads to renewal of surface contacting molecule leading to increase in mass transfer coefficient.

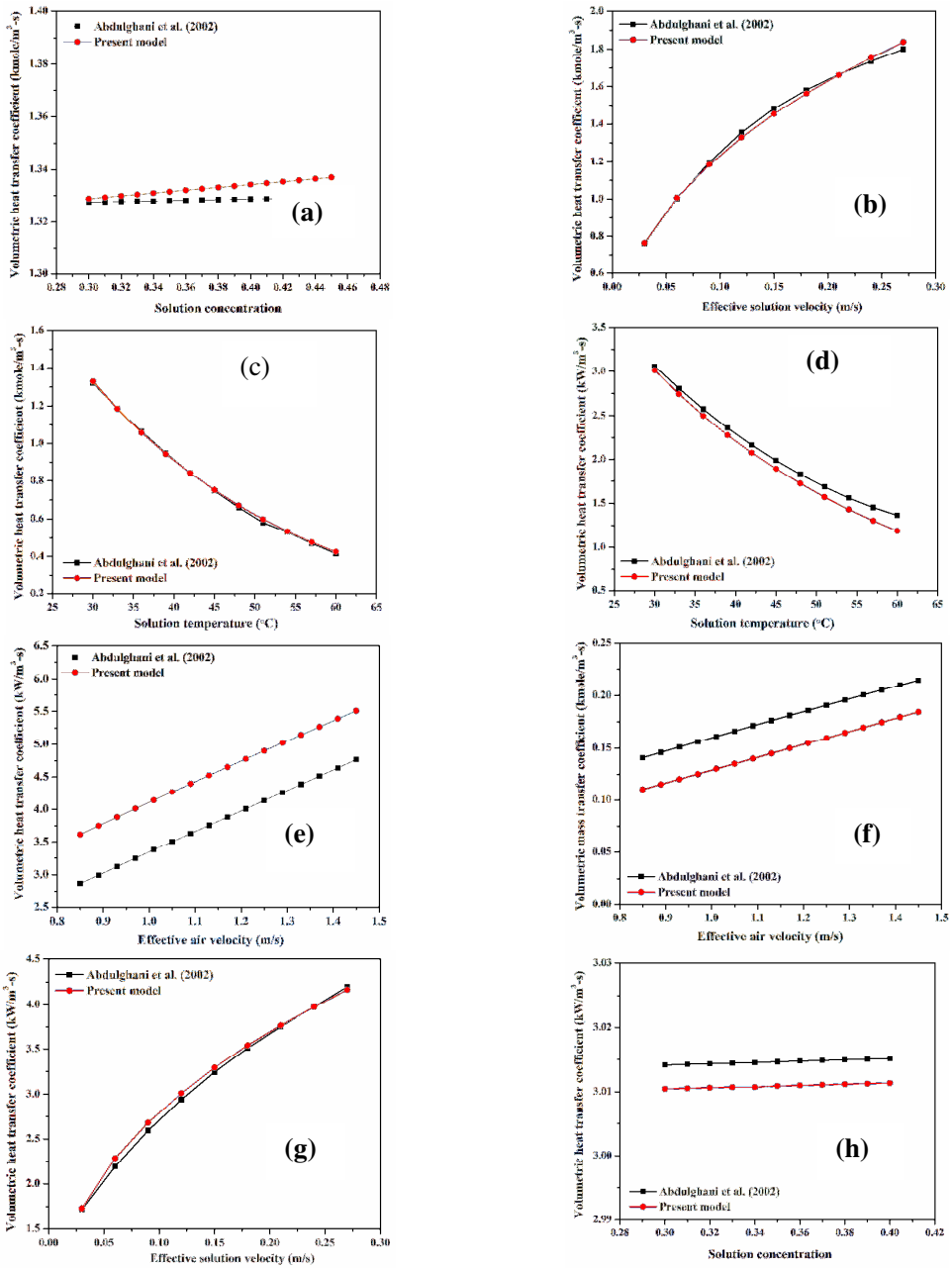

Figure 3 Validation of the volumetric heat and mass transfer coefficients by solution concentration , solution velocity, solution temperature, and air velocity

3.3.3 Variation of liquid volumetric mass transfer coefficient with liquid desiccant temperature

As the desiccant solution temperature increases it leads to weakening of desiccant the bond with water. This increases the pressure above the interface and hence the vapour pressure difference between the interface and air decreases, which leads to decrease in the potential for the mass transfer. This can be clearly seen in the following figure 3.C where the volumetric mass transfer coefficient is decreasing with the increase in desiccant temperature. The average error in the finding was around 0.8%.

3.3.4 Variation of liquid volumetric heat transfer coefficient with liquid desiccant temperature

The volumetric heat transfer coefficient is weak function of the desiccant temperature as it can be seen from the below figure 3.D. While predicting the volumetric heat transfer coefficient the effective air, liquid velocities were kept to be constant around 10.5 m/s, 0.12 m/s and concentration was kept to 40%.

The average error in predicting the volumetric heat transfer coefficient was around 5%. the model and paper values comparison is shown in figure 3.D. When the desiccant temperature increases it decreases the local temperature gradient and hence decreases the overall heat transfer coefficient.

3.3.5 Variation of volumetric heat transfer coefficient with effective air velocity

The volumetric heat transfer coefficients showed little variation form the original equation values. The average error in predicting the volumetric heat transfer coefficient was around 20% with the variation of the effective air velocity (0.85 m/s to 1.45 m/s). Figure 3.E shows the variation in the model values and the paper values. Increase in the air velocity will definitely improve the heat transfer coefficient in forced process. As the air speed increases so does the newer molecules come in contact with the surface hence, the volumetric heat transfer coefficient increases.

3.3.6 Variation of air volumetric mass transfer coefficient with effective air velocity

Here the air temperature was kept around the 25℃ with the effective velocity of the liquid was kept around 0.0066 m/s and the air velocity was varied from the 0.85-1.45 m/s. The average error in predicting the volumetric mass transfer coefficient was found to be around 21.5%. The concentration of the LiCl solution was around 40%. The variation in the predicted and paper values is shown in figure 3.F. As the air velocity increases so the slope of the variation in the pressure across the interface increases without utilizing the full potential of mass transfer which leads to increase in the more mass transfer. The interface will be supplied with new air and hence giving lesser time to interact, which corresponds to high starting potential near interface surface leading to increase in the mass transfer.

3.3.7 Variation of liquid volumetric heat transfer coefficient with effective liquid velocity

Increasing the velocity of the liquid increases the volumetric heat transfer coefficient. Here they have considered the variation of the liquid velocity to be in the range of 0.03 to 0.27 m/s. While calculating the effect; the air effective velocity was kept constant to around 10.5 m/s and the desiccant temperature was 30℃ with 40% concentration of LiCl solution. Figure 3.G shows the variation of the volumetric heat transfer coefficient with effective liquid velocity. The average error in the findings were around the 1.5%. As the liquid velocity increases it also increases the newer molecules contact with interface leading to effective heat transfer hence the liquid volumetric heat transfer coefficient increases with the liquid velocity.

3.3.8 Variation of liquid volumetric heat transfer coefficient with solution concentration

The effect of variation of concentration is negligible on volumetric heat transfer coefficient. Here they have considered the air and liquid effective velocities to be around 10.5 m/s and 0.12 m/s with 30℃ desiccant temperature. The average error in the findings were around 0.12%. Figure 3.H shows the volumetric heat transfer coefficient variation with solution concentration. This effect is related to the increase in the mass transfer in the liquid.

3.4 To optimize the mixture of desiccant solution by desirability approach based on statistics

The design expert 13.0 has been used for the optimization study. The inlet 14 dataset from the dehumidifier model was given input to design expert 13.0. For the given study the 10 points were allocated for the edge and 4 for the vertex. Concentration limits for LiCl is taken in the range of 30% to 40% and for water it is in the range of 60% to 70%. Total concentration constraint is kept to 100%. The R^2 is 1.0 and other statistical values are in acceptable range. The high F-value is desirable and has been achieved. The probability values are less than 0.0001 and hence the terms are in good shape and have significant impact on the equations provided. The following quartic equations can be used to determine the performance parameters (for definitions of performance parameters see [21]) in the given range of the input concentration. Where A, B are the weight fraction of the LiCl, H_2O concentration. Where constants a_1 to a_5 are listed in below Table 2.

Performance Parameter (MRR, ΔP, ε_{Lat}, LHR)= a_1*A + a_2*B + a_3*AB+ a_4*AB(A-B) + a_5*AB(A-B)^2

Table 2 Performance parameters coefficients obtained from of the RSM study

	a_1	a_2	a_3	a_4	a_5
MRR(g/s)	7.6143	0.872205	-14.71747	-12.40233	-13.7091
Effectiveness (fraction)	176.9862	32.91078	-416.314	-272.8532	-314.6611
LHR (fraction)	2.93577	0.436042	-3.44474	-4.60629	-2.64926
Pressure drop (Pa/m)	182.2855	164.224	-186.4073	-311.3105	-371.7384

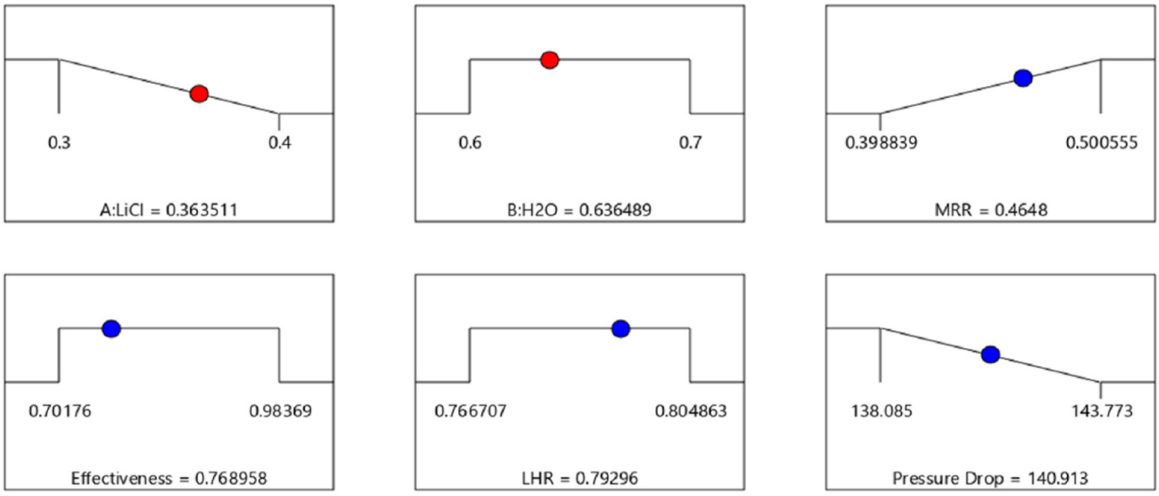

Figure 4. Desirability Ramp

3.4.1 Results of optimization for the desiccant solution mixture

The liquid flow rate is kept to 6.29 kg/m^2.s, mass flow ratio is kept around 5.29, temperature of air around 35℃ and desiccant temperature around 30℃ with inlet humidity to 0.0188 kg/kg of dry air. The RSM have produced the results with good accuracy. We have tried to minimize the LiCl concentration as its cost is high and along with that we have tried to reduce the pressure drop with maximization of the MRR. The results are shown in the desirability ramp figure 4. The optimized concentration for the solution is found to be 36.35% with it the MRR, ΔP, ε_{Lat}, LHR are 0.4648 g/s,140Pa/m, 76.89%, 79.29% respectively. The literature has shown good comparability with the results produced. The error is less than 0.84% in the prediction of the optimized concentration of LiCl solution [23].

4. Conclusions

Followings key conclusions can be drawn from the study:

- Here the finite difference method model includes the variation of the specific surface area of the packing material. The average error in the outlet specific humidity, concentration, air outlet temperature, desiccant outlet temperature determination is less than 7%, 0.35%, 4%, 4.2%, respectively.
- Pressure drop was calculated for Polypropylene structured packing for the LiCl desiccant solution. The calculated results have been compared with the literature data. The error in the pressure drop prediction was less than 2.5%. The calculation of pressure drop per unit length gives the best packing material as Mellapak 250Y for $CaCl_2$ desiccant solution.

- The liquid and air heat and mass transfer coefficients were calculated with error less than 2%. These equations for air heat and mass transfer can be used for further predictions with knowing effective velocities in the structure.
- The design of experiments is used for optimization of the concentration of the LiCl desiccant solution with central composite method. The optimized value of the performance parameters MRR, ΔP, ε_{Lat}, LHR at the optimized concentration of the solution at 36.35 % is found to be 0.4648 g/s, 140 Pa/m, 76.89%, 79.29 %, respectively.

Symbols and abbreviations

a_t	Total Specific surface area (m^2/m^3)		**Greek Symbol**
D_p	Equivalent diameter, m	ϵ	Void Fraction
D	Diffusivity (m^2/s)	σ	Density (kg/m^3)
g	Acceleration due to Gravity (m/s^2)	u	Dynamic viscosity (Pa.s)
F	F type mass transfer coefficient ($kmole/m^2.s$)	σ	Surface tension (N/m)
h	Volumetric heat transfer coefficient ($kW/K.m^3$)	ρ	Density (kg/m^3)
h_a	Static liquid holdup		**Subscripts**
K	Mass transfer coefficient ($kmole/m^2.s.Pa$)	L	Liquid
L	Liquid Flow rate ($kg/m^2.s$)	G	Gas
Re, Fr, We	Reynolds, Froude, Weber number	C	Critical
P	Pressure (Pa)	Sat	Saturation
R	Ideal gas constant(kJ/kmole.K)	t, tot	Total
T	Temperature in (°C)	E	Effective
x	Concentration in Fraction of weight	out	Outlet
Y	Specific humidity (kg/kg of dry air)	in	Inlet

References

[1] Sustainable TE and RI (TERI); NRDC (NRDC); I for G&. Improving Air Conditioners in India. 2018.

[2] Yang Z, Feng B, Ma H, Zhang L, Duan C, Liu B, et al. Analysis of Lower GWP and Flammable Alternative Refrigerants. Int J Refrig 2021. https://doi.org/10.1016/j.ijrefrig.2021.01.022.

[3] Nair V. HFO refrigerants: A review of present status and future prospects. Int J Refrig 2021;122:156–70. https://doi.org/10.1016/j.ijrefrig.2020.10.039.

[4] Saleh B. Energy and exergy analysis of an integrated organic Rankine cycle-vapor compression refrigeration system. Appl Therm Eng 2018;141:697–710. https://doi.org/10.1016/j.applthermaleng.2018.06.018.

[5] Ahmed SY, Gandhidasan P, Al-Farayedhi AA. Thermodynamic analysis of liquid desiccants. Sol Energy 1998;62:11–8. https://doi.org/10.1016/S0038-092X(97)00087-X.

[6] Fu HX, Liu XH. Review of the impact of liquid desiccant dehumidification on indoor air quality. Build Environ 2017;116:158–72. https://doi.org/10.1016/j.buildenv.2017.02.014.

[7] Girnik I, Yang T, Gordeeva L, Wang W, Ge T, Aristov Y. New adsorption method for moisture and heat exchange in ventilation systems in cold countries: Concept and mathematical simulation. Energies 2020;16. https://doi.org/10.3390/en13061386.

[8] Tokarev MM, Gordeeva LG, Grekova AD, Aristov YI. Adsorption cycle "heat from cold" for upgrading the ambient heat: The testing a lab-scale prototype with the composite sorbent CaClBr/silica. Appl Energy 2018;211:136–45. https://doi.org/10.1016/j.apenergy.2017.11.015.

[9] Factor HM, Grossman G. A packed bed dehumidifier/regenerator for solar air conditioning with liquid desiccants. Sol Energy 1980;24:541–50.

[10] Treybal RE. Mass Transfer Operations. 3rd ed. Rhode Island: McGRAW-HILL book company; 1981.

[11] Fumo N, Goswami DY. Study of an aqueous lithium chloride desiccant system: Air dehumidification and desiccant regeneration. Sol Energy 2002;72:351–61. https://doi.org/10.1016/S0038-092X(02)00013-0.

[12] Luo Y, Yang H, Lu L, Qi R. A review of the mathematical models for predicting the heat and mass transfer process in the liquid desiccant dehumidifier. Renew Sustain Energy Rev 2014;31:587–99. https://doi.org/10.1016/j.rser.2013.12.009.

[13] Pahlavanzadeh H, Nooriasl P. Experimental and Theoretical Study of Liquid Desiccant Dehumidification System by Using the Effectiveness Model. J Therm Sci Eng Appl 2012;4:1–9. https://doi.org/10.1115/1.4005210.

[14] Stichlmair J, Bravo JL, Fair JR. General model for prediction of pressure drop and capacity of countercurrent gas/liquid packed columns. Gas Sep Purif 1989;3:19–28. https://doi.org/10.1016/0950-4214(89)80016-7.

[15] Gandhidasan P. Prediction of pressure drop in a packed bed dehumidifier operating with liquid desiccant. Appl Therm Eng 2002;22:1117–27. https://doi.org/10.1016/S1359-4311(02)00031-5.

[16] Hanley B, Dunbobbin B, Bennett D. A Unified Model for Countercurrent Vapor/Liquid Packed Columns. 1. Pressure Drop. Ind Eng Chem Res 1994;33:1208–21. https://doi.org/10.1021/ie00029a017.

[17] Ortiz-Del Castillo JR, Guerrero-Medina G, Lopez-Toledo J, Rocha JA. Design of steam-stripping columns for removal of volatile organic compounds from water using random and structured packings. Ind Eng Chem Res 2000;39:731–9. https://doi.org/10.1021/ie990432m.

[18] Koronaki IP, Christodoulaki RI, Papaefthimiou VD, Rogdakis ED. Thermodynamic analysis of a counter flow adiabatic dehumidifier with different liquid desiccant materials. Appl. Therm. Eng., vol. 50, 2013, p. 361–73. https://doi.org/10.1016/j.applthermaleng.2012.06.043.

[19] Chung TW, Ghosh TK, Hines AL. Comparison between Random and Structured Packings for Dehumidification of Air by Lithium Chloride Solutions in a Packed Column and Their Heat and Mass Transfer Correlations. Ind Eng Chem Res 1996;35:192–8. https://doi.org/10.1021/ie940652u.

[20] Abdulghani A. Al-Farayedhi AA, Gandhidasan P, Al-Mutairi MA. Evaluation of heat and mass transfer coefficients in a gauze-type structured packing air dehumidifier operating with liquid desiccant. vol. 25. Dhahran 31261, Saudi Arabia: 2002.

[21] Bhowmik M, Muthukumar P, Anandalakshmi R. Experimental investigation on structured packed bed liquid desiccant dehumidifier: An optimal mixture design of experiments strategy. Int J Refrig 2021;122:232–44. https://doi.org/10.1016/j.ijrefrig.2020.11.006.

[22] Conde-Petit MR. Aqueous solutions of lithium and calcium chlorides: – Property formulations for use in air conditioning equipment design. M Conde Eng 2009:29.

[23] Wang H, Cheng Q, Feng W, Xu W. Experimental and theoretical research on the electrical conductivity of a liquid desiccant for the liquid desiccant air-conditioning system: LiCl aqueous solution. Int J Refrig 2018;91:189–98. https://doi.org/10.1016/j.ijrefrig.2018.04.025.